



# A Variable Stiffness Robotic Arm Using Linearly Actuated Compliant Parallel Guided Mechanism

R. Hu, V. Venkiteswaran, and H.-J. Su<sup>(✉)</sup>

Department of Mechanical and Aerospace Engineering,  
The Ohio State University, Columbus, OH, USA  
su. 298@osu.edu

**Abstract.** This paper details the mechanical design and control of a human safety robotic arm with variable stiffness, starting from conceptual design to prototype. The mechanism designed is based on parallel guided beam with a roller slider actuated by a power screw and a DC motor with an encoder for position feedback. Unlike conventional robotic systems that control the stiffness in joints, this design introduces compliance to the robotic arm link itself. By controlling the slider position, the effective length of the link can be adjusted to provide the necessary stiffness change. A PID position controller is employed and the position accuracy is experimentally evaluated. The stiffness variation of the prototype is validated by experiments and FEA simulation. The overall stiffness change achieved is 20-fold.

**Keywords:** Variable stiffness · Human-safe robot · Collaborative robot · Compliant mechanisms

## 1 Introduction

Collaborative robot or Co-robots [1] have been widely used in automotive industries and material handling. These co-robots are designed to work with human workers side by side. However safety has been a major concern and challenges. The current methods of addressing the safety are mostly by reducing execution speed upon detection of impact or proximity of human workers via force or vision sensors [2–4]. The main concern of this method is that the co-robot safety highly relies on the sensing system or requires initial contact between the operators and the robots. If any of the electronic modules fail, the co-robots may injure operators by accident.

An alternative method for addressing the safety is by mechanical design approach [5, 6]. The mechanical design based co-robot mainly focuses on reducing the stiffness of the mechanism. The use of variable stiffness or compliance has been introduced to co-robot designs. She *et al.* [7] and Avadhanula *et al.* [8] already discussed the importance of design methods in achieving the necessary stiffness change. The conventional approach is to manipulate the stiffness of robotic arm joint. Kobayashi [9] designed a variable stiffness joint driver to realize joint angle control. Bicchi *et al.* [10] developed a compliant nonlinear actuator to realize intrinsic safety of the robotic

system. Other methods in mechanical design of co-robot joints are energy-based or material oriented shown by Wolf *et al.* [11] and Chen *et al.* [12]. Introducing compliance to kinematic joints and actuators has been demonstrated as a major approach to achieve the stiffness change in mechanical design based co-robot research [13]. And our recent comparative study [14] showed that compliant links generally have a higher effect than compliant joints in reducing the maximum impact force.

The design presented in this work introduces variable compliance to the robotic arm link itself. The stiffness variation of the robotic arm is derived by controlling the effective length of the parallel guided mechanism. As a added contribution to existing designs, this paper provides a new solution for robot inherently safety with fewer actuators and simple control method.

## 2 Concept of the Design

The concept of the variable stiffness robotic arm design is based on the parallel guided beam, consisting of two single end-guided flexures with a rigid connection in between. Figure 1 shows the parallel guided mechanism with angular constraints at the free end.

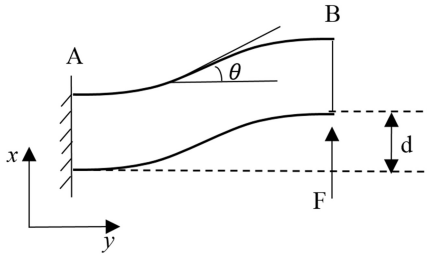


**Fig. 1.** Top view of parallel guided beam with free end constraints.

When a concentrated force  $F$  is applied at the free end, the angular deflection  $\theta$  of the beam at the tip is zero and the deflection along with direction of the force is  $d$ . The deflection in horizontal direction  $y$  is negligible. The stiffness of the beam is calculated as [15]:

$$k = \frac{24EI}{L^3} \quad (1)$$

In the equation above,  $E$  is the elastic modulus of the beam material, and  $I$  is the cross section moment of inertia of each beam.  $L$  is the effective beam length. The concept of the proposed design is to change the effective length of the parallel guided beam with fixed  $E$  and  $I$  to implement stiffness variation.

### 3 Prototype of the Robotic Arm Design

The design of the variable stiffness robotic arm is shown in Fig. 2. The arm has two parallel Al 7075 sheet flexures with a distance of 49.7 mm in between, each with a thickness of 0.79375 mm and height of 73.5 mm. The fixed end is designed to be the motor and transmission housing. A power screw with a lead of 4 mm is assembled through the slider. To allow the bending of the two flexures, a small nut featuring with grooves is added to the free end containing spherical balls as rolling supports. The section from the free end to the slider is the effective length and is free to move. The remainder of the arm is rigidly supported by the power screw. The two sheet flexures are constrained by linear bearings on the slider shaft, with retaining rings coupled as stoppers. The overall dimensions of the prototype are 406 mm  $\times$  95 mm  $\times$  104 mm and the total weight is 952 g. A timing belt transmission with teeth ratio of 19:21 was designed to drive the power screw.

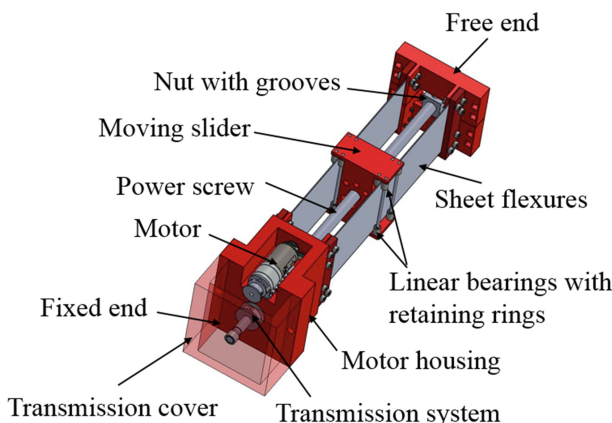
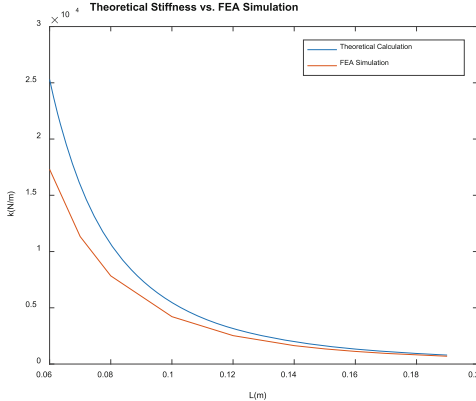


Fig. 2. CAD design of the variable stiffness robotic arm.

### 4 FEA Simulation

An FEA model was created for concept validation. The model used wire features and beam elements in a 2D planar workspace. There were two sections assigned in the FEA simulation. The two sheet flexures were assigned an elastic modulus of 71.7 GPa, for Al 7075. The connector at the free end was assumed to be rigid.

The boundary conditions applied at the fixed end were displacement  $U_1 = U_2 = UR_3 = 0$  in directions of  $x$ ,  $y$ , and the rotation around  $z$ -axis. At the slider position, the roller constraints were simulated as  $U_1 = 0$  in  $x$  direction. The linear displacement  $U_2$  in the axial direction and the rotational displacement  $UR_3$  around  $z$ -axis were not constrained. A concentrated force was applied in  $x$  direction at the free end and the tip deflection was recorded to calculate stiffness. The comparison between the stiffness simulation result and theoretical calculation is plotted in Fig. 3.



**Fig. 3.** FEA simulation stiffness result compared to theoretical calculation. L is the effective length of the beams.

## 5 Actuation Module and PID Control

The motor used in the prototype is a DC gear motor with an encoder which provided a feedback of motor shaft rotation. The primary objective was to control the motor shaft rotation steps to achieve effective length changes. The DC motor is controlled by an Arduino Uno microcontroller which has a maximum output of 5 V voltage and 20 mA current. The motor operating conditions are 6.5 V voltage with 200 mA current. Thus an external power and a dual motor drive were included in the circuit. The circuit wiring schematic is shown in Fig. 4.

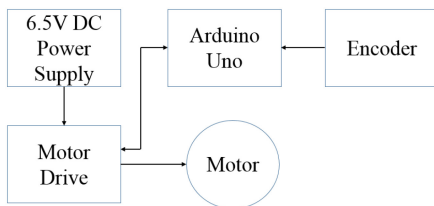


**Fig. 4.** Wiring schematic of Arduino circuit.

The motor driver communicates with the Arduino Uno board and provides the operating voltage to the DC motor. The Arduino controller generates PWM signals according to the feedback from the encoder. A conventional PID controller was used to directly control the armature voltage input according to the motor step error between the desired and actual positions. Similar strategy of PID closed loop position control has been discussed in literature [16]:

$$e(k) = Y_d(k) - Y(k) \quad (2)$$

$$PID(k) = K_p e(k) + K_d (e(k) - e(k-1)) / t_{loop} + K_t t_{loop} \sum_{i=0}^{k-1} e(i) \quad (3)$$

$$PWM\_val(k) = PID(k) \quad (4)$$

$Y(k)$  is the actual step of the motor armature.  $Y_d(k)$  is the desired step value at  $k^{th}$  time step. The PID controller continuously calculates the position error  $e(k)$  and applies a correction.  $PWM\_val(k)$  is the duty ratio of the pulse-width modulation. The parameters  $K_p$ ,  $K_i$  and  $K_d$  were tuned until the steady state error of the motor shaft position was small by observation.

## 6 Prototype Performance Evaluation

The slippage and backlash of the transmission introduced proportional error to the slider position output. The system was calibrated by compensating the error with a gain added to the controller. The position accuracy was tested using a digital caliper. Figure 5 shows the experimental setup.

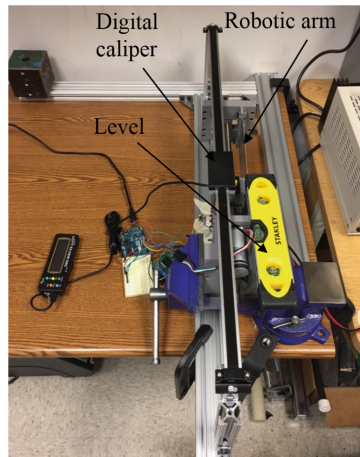


**Fig. 5.** Experimental setup of PID position calibration.

The digital caliper was arranged parallel to the length of the robotic arm and attached to the slider via a hook. When the slider moved to a desired position, the digital caliper recorded the actual travelling distance. The increment of the motor shaft rotation was broken into half a revolution  $n$  and the slope of the desired travelling distance vs.  $n$  should be 2 mm. Figure 6 shows the test result after calibration in forward direction with PID position calibration as an example. The slope of the actual travelling distance vs.  $n$  is around 1.997 mm in both forward and backward directions which matches well with the desired value.

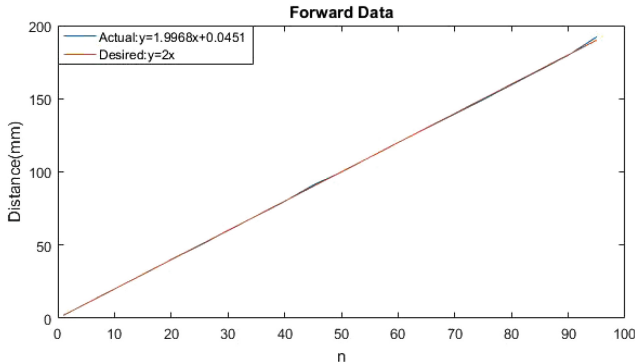


**Fig. 6.** PID position control forward accuracy test results.

A static and a dynamic stiffness test were performed on the prototype. The experimental setup is shown in Fig. 7. The measurement system consisted of a single axis force sensor and a displacement sensor arranged in parallel. The robotic arm was clamped in a stationary fixture with no support at the free end.

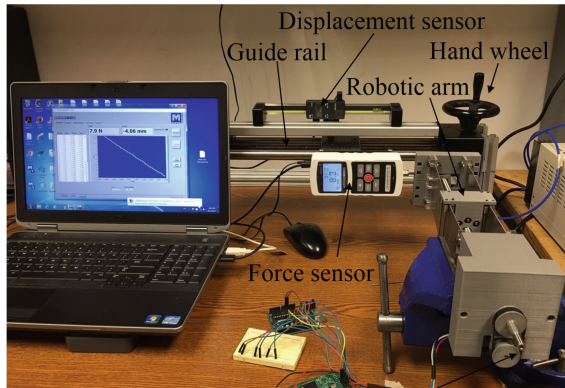


**Fig. 7.** Stiffness test experiment setup for prototype.

In the static stiffness test, the motor drove the slider to the desired position and a continuously increasing displacement input was provided at the tip position after the slider completely stopped. The test was performed for 16 positions of the slider, repeated 3 times. The force-displacement data was fit into a linear curve to calculate the slope, which is the experimental stiffness. The dynamic stiffness test was conducted with the slider running at a constant mode. The dynamic stiffness test was performed at four fixed tip deflections from 0.5 mm to 2 mm. Figure 8 shows the experimental results compared with the Theoretical stiffness calculation.

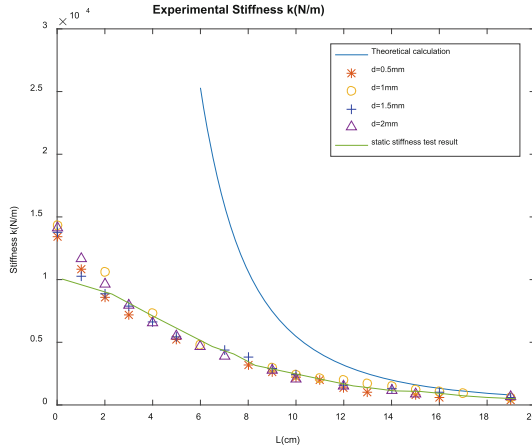


**Fig. 8.** Stiffness comparison of prototype experimental results and theoretical calculation.

Theoretically the stiffness goes to infinity when the effective length is zero, which is not realistic on the physical model. The experimental stiffness of the prototype is close to theoretical calculation at high effective lengths but starts deviating significantly from  $L_{eff} = 8$  cm. The error was introduced by the slippage between subassemblies in the prototype and deformation of other parts which were 3D printed by PLA. The angular displacement at the tip and the longitudinal deformation of free end were not negligible under large load. The dynamic stiffness test result is overall consistent with the static test except for the values at  $L_{eff} = 0.21$  cm due to inertia of the slider. The maximum static stiffness is 10048.67 N/m and the minimum value is 499.85 N/m, showing that the current design is capable of stiffness change by 20 fold.

## 7 Conclusions

In this paper, we present the mechanism design of a variable stiffness robotic arm with two parallel guided beams. The stiffness change is enabled by changing the effective length of beams through a roller carriage which is actuated by a screw drive and an electric motor. Our experimental tests show that the design can achieve a stiffness change ratio of 20 times. By a closed-loop PID position control, we successfully achieved an accurate and stable stiffness variation.

For future work, the DC motor was selected conservatively for a large torque, which can be replaced by one with higher RPM. A lighter power screw with larger lead and smaller pitch diameter should be considered. The overall design can be more compact with reduced weight and size. The dynamic performance of impact load must be tested on this design as a criterion to evaluate impact injuries. Also, the robotic arm designed can be developed into stiffness variation in multiple directions by cascading integration.

## References

- Colgate, J.E., Edward, J., Peshkin, M.A., Wannasuphprasit, W.: Cobots: Robots For Collaborative With Human Operators (1996)
- Zhang, J., Zhuang, L., Wang, Y., Zhou, Y., Meng, Y., Hua, G.: An egocentric vision based assistive co-robot. In: 2013 IEEE 13th International Conference on Rehabilitation Robotics (ICORR), Seattle, WA, pp. 1–7 (2013)
- Lumelsky, V.J., Cheung, E.: Real-time collision avoidance in teleoperated whole-sensitive robot arm manipulators. *IEEE Trans. Syst. Man Cybern.* **23**(1), 194–203 (1993)
- Liang, P., Ge, L., Liu, Y., Zhao, L., Li, R., Wang, K.: An augmented discrete-time approach for human-robot collaboration. *Discret. Dyn. Nat. Soc.* **2016**, 13 (2016). Article ID 9126056
- She, Y., Meng, D., Shi, H., Su, H.-J.: Dynamic modeling of a 2D compliant link for safety evaluation in human-robot interactions. In: 2015 IEEE/RSJ International Conference on Intelligent Robots and System (IROS), pp. 3759–3764 (2015)
- She, Y., Su, H.-J., Hurd, C.J.: Shape optimization of 2D compliant links for design of inherently safe robots. In: The ASME 2015 International Design Engineering Technical Conferences and Computers and Information in Engineering Conference, Boston, MA (2015). V05BT08A004
- She, Y., Su, H.-J., Lai, C., Meng, D.: Design and prototype of a tunable stiffness arm for safe human-robot interaction. In: ASME 2016 International Design Engineering Technical Conferences and Computers and Information in Engineering Conference, Charlotte, NC (2016). p. V05BT07A063
- Avadhanula, S., Fearing, R.: Flexure design rules for carbon fiber microrobotic mechanism. In: Proceedings of the 2005 International Conference on Robotics and Automation, 2005. ICRA 2005, pp. 1579–1584 (2005)
- Kobayashi, J., Okumura, K., Watanabe, Y., Suzuki, N.: Development of variable stiffness joint drive module and experimental results of joint angle control. In: Proceedings of the Fifteenth International Symposium on Artificial Life and Robotics, pp. 946–949 (2010)
- Bicchi, A., Tonietti, G., Piaggio, E.: Design, realization and control of soft robot arms for intrinsically safe interaction with humans. In: Proceedings of IARP/RAS Workshop on Technical Challenges for Dependable Robots in Human Environments, pp. 70–87 (2002)
- Wolf, S., Eiberger, O., Hirzinger, G.: The DLR FSJ: energy based design of a variable stiffness joint. In: 2011 IEEE International Conference on Robotics and Automation, Shanghai, pp. 5082–5089 (2011)
- Chen, Y., Yu, M., Bruck, H.A., Smela, E.: Stretchable touch-sensing skin over padding for co-robots. *Smart Mater. Struct.* **25**(5), 055006 (2016)
- Tsagarakis, N.G., Morfey, S., Medrano Cerdá, G., Zhibin, L., Caldwell, D.G.: COMpliant huMANoid COMAN: optimal joint stiffness tuning for modal frequency control. In: 2013 IEEE International Conference on Robotics and Automation, Karlsruhe, pp. 673–678 (2013)
- Howell, L.L.: Compliant Mechanisms. Wiley, New York (2001)
- She, Y., Meng, D., Cui, J., Su, H.-J.: On the impact force of human-robot interaction: joint compliance vs. link compliance. In: 2017 IEEE International Conference on Robotics and Automation (ICRA), pp. 6718–6723 (2017)
- Palm, W.: System Dynamics. McGraw-Hill Education, New York (2013)